

# A Method for Improving Simulation of PNA Teleconnection Interannual Variation in a Climate Model

LI Zhong-Xian<sup>1,2</sup>, ZHOU Tian-Jun<sup>2</sup>, SUN Zhao-Bo<sup>1</sup>, CHEN Hai-Shan<sup>1</sup>, and NI Dong-Hong<sup>1</sup>

<sup>1</sup> Key Laboratory of Meteorological Disaster of Ministry of Education, Nanjing University of Information Science & Technology, Nanjing 210044, China

<sup>2</sup> State Laboratory of Numerical Modeling for Atmospheric Sciences and Geophysical Fluid Dynamics (LASG), Institute of Atmospheric Physics (IAP), Chinese Academy of Sciences, Beijing 100029, China

Received 8 December 2010; revised 28 December 2010; accepted 29 December 2010; published 16 March 2011

**Abstract** The climate modeling community has been challenged to develop a method for improving the simulation of the Pacific-North America (PNA) teleconnection pattern in climate models. The accuracy of PNA teleconnection simulation is significantly improved by considering mesoscale convection contributions to sea surface fluxes. The variation in the PNA over the past 22 years was simulated by the Grid Atmospheric Model of IAP LASG version 1.0 (GAMIL1.0), which was guided by observational SST from January 1979 to December 2000. Results show that heating in the tropical central-eastern Pacific is simulated more realistically, and sea surface latent heat flux and precipitation anomalies are more similar to the reanalysis data when mesoscale enhancement is considered during the parameterization scheme of sea surface turbulent fluxes in GAMIL1.0. Realistic heating in the tropical central-eastern Pacific in turn significantly improves the simulation of interannual variation and spatial patterns of PNA.

**Keywords:** sea surface turbulent flux parameterization, PNA, climate simulation

**Citation:** Li, Z.-X., T.-J. Zhou, Z.-B. Sun, et al., 2011: A method for improving simulation of PNA teleconnection interannual variation in a climate model, *Atmos. Oceanic Sci. Lett.*, **4**, 86–90.

## 1 Introduction

The Pacific-North America (PNA) teleconnection presents one of the most prominent large-scale patterns of atmospheric low-frequency variability in the northern extratropics. It is driven by oscillations in geopotential height over the Pacific Ocean and across the North American continent (Bladé, 1999; Stoner et al., 2009). The El Niño-Southern Oscillation (ENSO) phenomenon involves large SST anomalies in the eastern tropical Pacific, which lead to substantial anomalies in evaporation and the reorganization of cumulus convection through the Pacific. The resultant deep anomalous tropical heat source produces a Rossby wave response, which emanates into the extratropics, particularly the Pacific-North America regions (Straus and Shukla, 2002). The PNA tends to be positive during El Niño events, and its time series illustrates an increasingly positive trend in recent years, which

follows SST trends for the central equatorial Pacific (Trenberth et al., 1998). The PNA spatial pattern is realistically simulated by a three level quasi-geostrophic model (Corti et al., 1997), which provides much better forecasting for strong-amplitude ENSO years than for normal years (Derome et al., 2005). Using 22 of the coupled atmosphere-ocean general circulation model (AOGCM) simulations submitted to the Intergovernmental Panel on Climate Change (IPCC) Fourth Assessment Report (AR4), Stoner et al. (2009) found that only two AOGCMs were relatively successful at simulating PNA time series, although almost all AOGCMs were able to simulate a recognizable PNA spatial pattern. Therefore, simulation of the PNA is one of the most important and challenging tasks of climate research.

Air-sea interaction plays a key role in the Earth's climate, especially over tropical oceans (Mondon and Redelsperger, 1998). Variations in Pacific SSTs and precipitation patterns have profound climate implications for the tropics and, most likely, for the extratropics (Collins et al., 1997). Variations in SST modulate convective activity, and hence the diabatic forcing, through the evaporation from the ocean surface. Thus, general circulation models' abilities to represent tropical circulations and to faithfully simulate the sensitivity of the atmosphere to SST variations depend upon surface flux parameterization (Miller et al., 1992; Palmer et al., 1992; Webster and Lukas, 1992; Brunke et al., 2003).

Atmospheric and oceanic general circulation models (GCMs) parameterize surface fluxes using the bulk aerodynamic method. In general, current schemes use formulae based on local measurements and assume horizontally homogeneous parameters over the grid scale, but this assumption is not necessarily true (Mondon and Redelsperger, 1998). It has been shown that the effects of atmospheric mesoscale convection lead to enhanced surface fluxes (Saxen and Rutledge, 1998). Based on Tropical Ocean Global Atmosphere (TOGA) array mooring data, Esbensen and McPhaden (1996) found that mesoscale enhancement of evaporation can reach 30% of the total evaporation. Miller et al. (1992) used the European Centre for Medium-Range Weather Forecasts' (ECMWF) model to reveal model sensitivity to air-sea flux parameterization at low wind speeds. After considering the effect of free convection on surface fluxes, the interannual, seasonal, and intraseasonal variability of general circulations were

more realistically simulated. The same results were seen using the Community Atmospheric Model version 3 (CAM3) (Li et al., 2009).

The Grid Atmospheric Model of Institute of Atmospheric Physics (IAP), the State Laboratory of Numerical Modeling for Atmospheric Sciences and Geophysical Fluid Dynamics (LASG) version 1.0 (GAMIL1.0) is a grid-point atmospheric general circulation model (AGCM) developed by IAP LASG, Chinese Academy of Sciences (CAS). It is widely used for climate simulations on interdecadal and interannual timescales (Li et al., 2007; Zhou et al., 2009a–c; Kucharski et al., 2009). However, weak sensitivity to changes in sea surface temperatures has been observed during the use of GAMIL1.0 (Scaife et al., 2009). This paper employs improved parameterization of GAMIL1.0 by considering the effect of mesoscale enhancement on sea surface heat fluxes. The impact is highly beneficial because it greatly improves the interannual variability and spatial pattern of the PNA.

The remainder of the paper is organized as follows: the experimental design and observed data used to evaluate the model results are described in section 2; section 3 presents the simulation of the interannual variability and spatial pattern of PNA; section 4 discusses the mechanism responsible for the effect of mesoscale enhancement on PNA simulation; and the conclusion is given in section 5.

## 2 Experimental design and data

### 2.1 Model and experimental design

GAMIL1.0 employs a horizontal resolution of  $2.8^\circ \times 2.8^\circ$  and 26 levels of vertical resolution. The model uses a dynamical core developed by Wang et al. (2004) and physical packages from the Community Atmospheric Model Version 2 (CAM2) of the National Center for Atmospheric Research (NCAR; Collins et al., 2003). The parameterization scheme (GAMIL scheme) of sea surface turbulent fluxes in GAMIL1.0 was improved by considering the contribution of the mesoscale convection to sea surface fluxes (Zeng et al., 2002; Li et al., 2011). The new parameterization scheme is named the GAMIL\_rev scheme. The interannual variability of general circulation is simulated by the GAMIL1.0 model by using observational SST data with the original parameterization scheme (GAMIL scheme) and the GAMIL\_rev scheme of sea surface turbulent fluxes.

### 2.2 Data

Observed data used in this paper include the National Oceanic and Atmospheric Administration's (NOAA) extended reconstruction SST data (Smith and Reynolds, 2003), the surface latent heat flux and 500 hPa geopotential height fields data obtained from the 40-yr ECMWF Re-Analysis (ERA40; Uppala et al., 2005) and the Climate Prediction Center Merged Analysis of Precipitation (CMAP; Xie and Arkin, 1996) data, spanning from January 1979 to December 2000. The horizontal resolution of SST is  $2^\circ \times 2^\circ$ , the resolution of geopotential height and precipitation is  $2.5^\circ \times 2.5^\circ$  and the resolution of surface

latent heat flux is a T62 Gaussian grid.

The period of analysis considered in this study spans the boreal winter season during the months of December, January, and February (DJF) from 1979–2000; for example, the 1980 winter represents December 1979, January 1980, and February 1980, and the 1979 winter consists of January 1979 and February 1979.

## 3 Interannual variability and spatial pattern of PNA teleconnection analysis

Following Horel and Wallace (1981), the PNA index is defined as:

$$\text{PNA} = \frac{1}{4} [ Z^*(20^\circ\text{N}, 160^\circ\text{W}) - Z^*(45^\circ\text{N}, 165^\circ\text{W}) + Z^*(55^\circ\text{N}, 115^\circ\text{W}) - Z^*(30^\circ\text{N}, 85^\circ\text{W}) ],$$

where, for example,  $Z^*(20^\circ\text{N}, 160^\circ\text{W})$  represents a normalized departure of a particular season from the mean 500 geopotential height at  $20^\circ\text{N}$ ,  $160^\circ\text{W}$ . Figure 1 depicts the simulated and observed winter PNA index from 1979 to 2000. GAMIL1.0 fails to simulate the interannual variability of the PNA during 1980s (Fig. 1). After considering the effect of the mesoscale convection on sea surface fluxes, the model performs better at capturing interannual variability in the PNA. The correlation coefficient between GAMIL (GAMIL\_rev) scheme simulated and observed PNA indices is 0.45 (0.68). These relationships are statistically significant at 95% and 99% confidence levels, respectively. Our results indicate that the GAMIL\_rev scheme can simulate the PNA index better than the GAMIL scheme.

To analyze the simulation of PNA spatial patterns, Fig. 2 provides regression coefficients for anomalous 500 hPa geopotential heights extracted from ERA40 data and the GAMIL and GAMIL\_rev scheme simulations against PNA indices from ERA40 data. In Fig. 2a, over a 500 hPa geopotential height field, the regression coefficients are 10 gpm and 40 gpm for the subtropical North Pacific and northwestern North America, respectively, and  $-80$  gpm and  $-20$  gpm for the Northeast Pacific and southwestern North America, respectively. It is in this way that four anomalous centers are located over the North Pacific and across North America, which is representative of the typical PNA teleconnection pattern. Figure 2b shows that

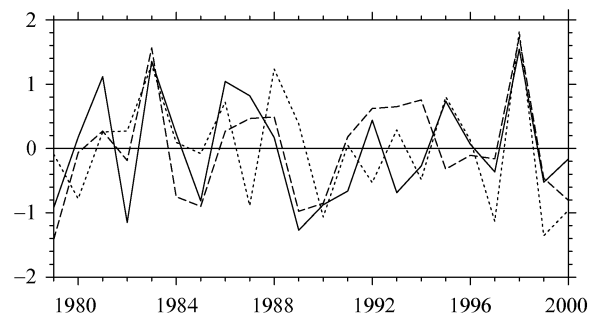


**Figure 1** Interannual variations in the winter PNA index. The solid line represents ERA40 data, the dotted line represents the GAMIL scheme simulation, and the dashed line represents the GAMIL\_rev scheme simulation.

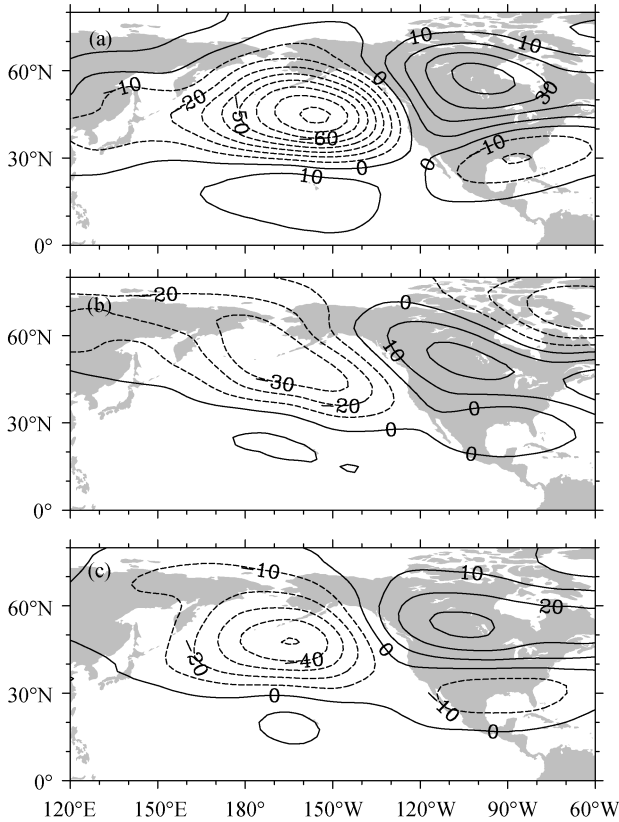


**Figure 2** Regression coefficients for winter 500 hPa geopotential height anomalies (gpm) from (a) ERA40 data, (b) GAMIL scheme simulations, and (c) GAMIL\_rev scheme simulations against PNA indices from ERA40 data.

the spatial features of the PNA pattern can be simulated by GAMIL1.0, but the simulated four anomalous centers are weaker than those from ERA40. Further, Fig. 2c shows that the four anomalous centers simulated by GAMIL\_rev are closer to those from ERA40.

#### 4 Mechanism analysis

Why is PNA simulation significantly improved by the GAMIL\_rev scheme? Tropical rainfall is important to the hydrological cycle. Three-fourths of the energy that drives atmospheric wind circulation comes from the latent heat released by tropical precipitation (Kummerow et al., 2000). Therefore, the performance of interannual tropical Pacific precipitation simulations for winter were analyzed. Figure 3 shows the regression patterns of anomalous tropical Pacific precipitation with the SST anomaly for the Niño3 region. Precipitation increased (decreased) over the central-eastern Pacific (western and subtropical Pacific) when the SST anomaly in the Niño3 region was positive (Fig. 3a). The simulated precipitation over central-eastern Pacific was lower than that reported by CMAP. The rate of precipitation reported by CMAP was  $5 \text{ mm d}^{-1}$ , whereas it was simulated to be less than  $4 \text{ mm d}^{-1}$  by both simulation schemes (Figs. 3b and 3c). This difference indicates that latent heat release over the tropical Pacific is not simulated as well by GAMIL1.0. However, precipitation rates over the tropical Pacific are simulated

more reasonably by the GAMIL\_rev scheme than the GAMIL scheme. In the tropical atmosphere, anomalous SSTs force anomalies in convection and large-scale overturning, with subsidence in the descending branch of the local Hadley circulation. The resulting strong upper tropospheric divergence in the tropics and convergence in the subtropics act as a Rossby wave source (Trenberth et al., 1998). In response to enhanced tropical heating during an El Niño event, the divergence in the tropics and convergence in the subtropics are strengthened, leading to an enhanced PNA teleconnection pattern through atmospheric Rossby wave propagation. Therefore, tropical heating plays a key role in reproducing the PNA teleconnection pattern. As discussed above, after taking into account the contribution of mesoscale enhancement to the air-sea surface fluxes, tropical precipitation and latent heat release are simulated more reasonably by GAMIL1.0, which in turn improves simulation of the interannual variability in the PNA.

To further verify the enhancement-effect of heating over the Pacific, Fig. 4 gives the regression coefficients for winter surface latent heat flux anomalies resulting from comparison of ERA40 data, and GAMIL and GAMIL\_rev scheme simulations to PNA indices calculated from ERA40 data. Figure 4a shows that the regression coefficients are positive over the tropical central-eastern Pacific with a maximum of  $15 \text{ W m}^{-2}$ . This pattern indicates that enhanced heating over the central-eastern Pacific significantly contributes to the intensity of the PNA teleconnection pattern. The regression coefficients are positive over the North Pacific region and

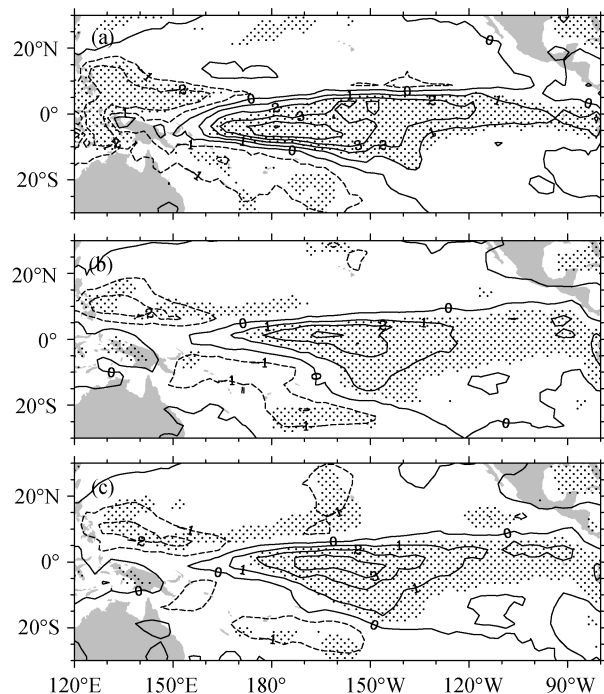


**Figure 3** Regression coefficients for winter tropical Pacific precipitation rates ( $\text{mm d}^{-1}$ ) from (a) CMAP data, (b) GAMIL scheme simulations, and (c) GAMIL\_rev scheme simulations against the SSTA in the Niño3 region. Areas with dots denote that the significance level (0.01) was exceeded.

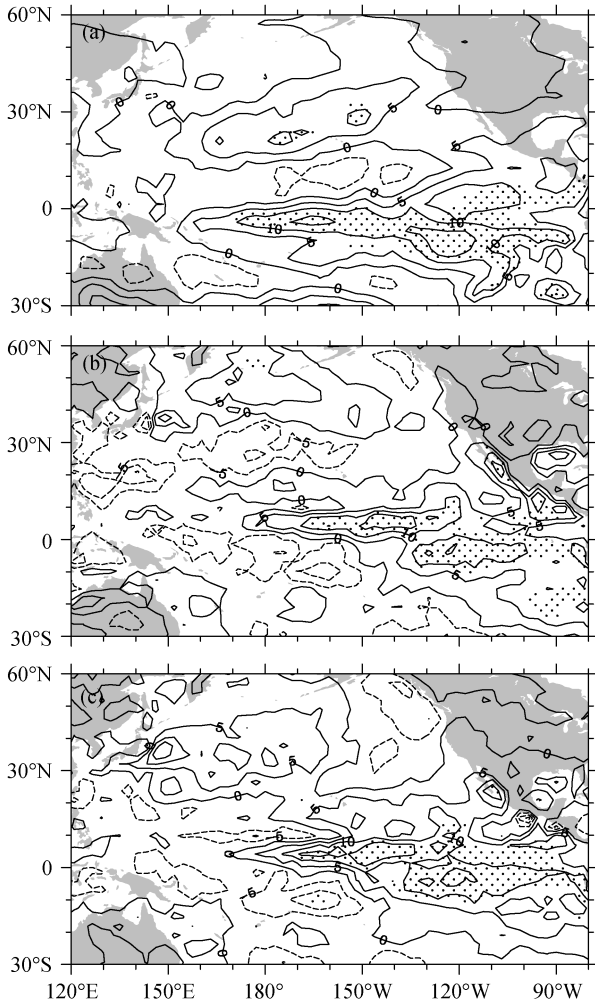


**Figure 4** Regression coefficients for winter surface latent heat flux ( $\text{W m}^{-2}$ ) anomalies from (a) ERA40 data, (b) GAMIL scheme simulations, and (c) GAMIL\_rev scheme simulations against PNA indices calculated from ERA40 data. Areas with dots denote that the significance level (0.01) was exceeded.

the Kuroshio region. When Fig. 4a is compared to Fig. 4b it becomes apparent that the latent heat fluxes simulated by GAMIL1.0 are lower than those from ERA40 for the tropical central-eastern Pacific and the North Pacific; and the GAMIL1.0 simulated latent heat flux is negative for the Kuroshio region, which is the opposite of the ERA40 results. After considering the mesoscale enhancement, the capability to simulate latent heat flux over the tropical central-eastern Pacific is significantly improved, and the simulated latent heat fluxes over the North Pacific and the Kuroshio region are also close to the ERA40 data (Fig. 4c).

## 5 Conclusions

To improve the accuracy of PNA simulation, mesoscale convection contributions to sea surface fluxes are considered as a component of the air-sea turbulent flux parameterization scheme of GAMIL model, named the GAMIL\_rev scheme. The interannual variability of general circulation is simulated by the GAMIL1.0 model using the

original parameterization scheme (GAMIL scheme) and GAMIL\_rev scheme of sea surface turbulent fluxes, which is achieved by the use of observed SST data. Results show that consideration of mesoscale enhancement in the scheme allows improved simulation of interannual variations in the intensity and phases of PNA teleconnection patterns by GAMIL1.0; the simulated PNA intensity during El Niño years is very close to that of ERA40 during the winter. The correlation coefficients resulting from the comparison of observed and simulated PNA intensities increased from 0.45 to 0.68 when the GAMIL and the GAMIL\_rev schemes were used, respectively. Consideration of mesoscale enhancement in the scheme also resulted in a more reasonable simulation of the response of precipitation to SST in the tropical central-eastern Pacific so that the sea surface latent heat flux anomaly was more similar to the reanalysis data. Inclusion of realistic heating in the tropical central-eastern Pacific significantly improved simulations of interannual variations and spatial patterns of PNA. Improvements in PNA simulation result in more accurate predictions of sea surface heat flux for the mid-latitude North Pacific.

**Acknowledgements.** The authors thank Dr. Lijuan LI, Dr. Qing BAO, and Dr. Bo WU for their helpful suggestions on GAMIL model, and the anonymous reviewers for their constructive reviews of the manuscript. This research was jointly supported by the National Natural Science Foundation of China under Grants 40905045 and 40821092, the Open Project for LASG-IAP-CAS, the Study Project of Jiangsu Provincial 333 High-level Talents Cultivation Programme, the Foundation of Key Laboratory of Meteorological Disaster of Ministry of Education under Grant KLME05001, and the Project Funded by the Priority Academic Programme Development of Jiangsu Higher Education Institutions.

## References

- Bladé, I., 1999: The influence of midlatitude ocean-atmosphere coupling on the low-frequency variability of a GCM. Part II: Interannual variability induced by tropical SST forcing, *J. Climate*, **12**, 21–45.
- Brunke, M. A., C. W. Fairall, and X.-B. Zeng, 2003: Which bulk aerodynamic algorithms are least problematic in computing ocean surface turbulent fluxes? *J. Climate*, **16**, 619–635.
- Collins, W. D., P. J. Rasch, B. A. Boville, et al., 2003: *Description of the NCAR Community Atmosphere Model (CAM2.0)*, NCAR Tech. Note, NCAR/TN-464+STR, Boulder, Colorado, 171pp.
- Collins, W. D., J. Wang, J. T. Kiehl, et al., 1997: Comparison of tropical ocean-atmosphere fluxes with the NCAR community climate model CCM3, *J. Climate*, **10**, 3047–3058.
- Corti, S., A. Giannini, S. Tibaldi, et al., 1997: Patterns of low-frequency variability in a three-level quasi-geostrophic model, *Climate Dyn.*, **13**, 883–904.
- Derome, J., H. Lin, and G. Brunet, 2005: Seasonal forecasting with a simple general circulation model: Predictive skill in the AO and PNA, *J. Climate*, **18**, 597–609.
- Esbensen, S. K., and M. J. McPhaden, 1996: Enhancement of tropical ocean evaporation and sensible heat flux by atmospheric mesoscale systems, *J. Climate*, **9**, 2307–2325.
- Horel, J. D., and J. M. Wallace, 1981: Planetary scale atmospheric phenomena associated with the Southern Oscillation, *Mon. Wea. Rev.*, **109**, 813–829.
- Kucharski, F., A. A. Scaife, J. H. Yoo, et al., 2009: The CLIVAR C20C project: Skill of simulating Indian monsoon rainfall on interannual to decadal timescales. Does GHG forcing play a role?

- Climate Dyn.*, **33**, 615–627, doi:10.1007/s00382-008-0462-y.
- Kummerow, C., J. Simpson, O. Thiele, et al., 2000: The status of the Tropical Rainfall Measuring Mission (TRMM) after two years in orbit, *J. Appl. Meteor.*, **39**, 1965–1982.
- Li, L.-J., B. Wang, and T.-J. Zhou, 2007: Impacts of external forcing on the 20th century global warming, *Chinese Sci. Bull.* (in Chinese), **52**, 1820–1825.
- Li, Z.-X., Z.-B. Sun, H.-S. Chen, et al., 2009: Improvement of sea surface turbulent fluxes parameterization scheme in CAM3 and its impact on climate simulation, *Acta Meteor. Sinica* (in Chinese), **67**, 1101–1112.
- Li, Z.-X., T.-J. Zhou, Z.-B. Sun, et al., 2011: Improvement of sea surface turbulent fluxes parameterization scheme in GAMIL and its impact on simulation of interannual variations of atmospheric circulation, *Chinese J. Atmos. Sci.* (in Chinese), **35**, 311–325.
- Miller, M. J., A. C. M. Beljaars, and T. N. Palmer, 1992: The sensitivity of the ECMWF model to the parameterization of evaporation from the tropical oceans, *J. Climate*, **5**, 418–434.
- Mondon, S., and J. L. Redelsperger, 1998: A study of a fair weather boundary layer in TOGA-COARE: Parameterization of surface fluxes in large scale and regional models for light wind conditions, *Bound.-Layer Meteor.*, **88**, 47–76.
- Palmer, T. N., Č. Branković, P. Viterbo, et al., 1992: Modeling interannual variations of summer monsoons, *J. Climate*, **5**, 399–417.
- Saxen, T. R., and S. A. Rutledge, 1998: Surface fluxes and boundary layer recovery in TOGA COARE: Sensitivity to convective organization, *J. Atmos. Sci.*, **55**, 2763–2781.
- Scaife, A. A., F. Kucharski, C. K. Folland, et al., 2009: The CLIVAR C20C project: Selected twentieth century climate events, *Climate Dyn.*, **33**, 603–614, doi:10.1007/s00382-008-0451-1.
- Smith, T. M., and R. W. Reynolds, 2003: Extended reconstruction of global sea surface temperatures based on COADS data (1854–1997), *J. Climate*, **16**, 1495–1510.
- Stoner, A. M. K., K. Hayhoe, and D. J. Wuebbles, 2009: Assessing general circulation model simulations of atmospheric teleconnection patterns, *J. Climate*, **22**, 4348–4372.
- Straus, D. M., and J. Shukla, 2002: Does ENSO force the PNA? *J. Climate*, **15**, 2340–2358.
- Trenberth, K. E., G. W. Branstator, D. Karoly, et al., 1998: Progress during TOGA in understanding and modeling global teleconnections associated with tropical sea surface temperatures, *J. Geophys. Res.*, **103**(C7), 14291–14324.
- Uppala, S. M., P. W. Kållberg, A. J. Simmons, et al., 2005: The ERA-40 re-analysis, *Quart. J. Roy. Meteor. Soc.*, **131**, 2961–3012.
- Wang, B., H. Wan, Z.-Z. Ji, et al., 2004: Design of a new dynamical core for global atmospheric models based on some efficient numerical methods, *Sci. China-Math.*, **47**, 4–21.
- Webster, P. J., and R. Lukas, 1992: TOGA COARE: The coupled ocean-atmosphere response experiment, *Bull. Amer. Meteor. Soc.*, **73**, 1377–1416.
- Xie, P., and P. A. Arkin, 1996: Analyses of global monthly precipitation using gauge observations, satellite estimates, and numerical model predictions, *J. Climate*, **9**, 840–858.
- Zeng, X., Q. Zhang, D. Johnson, et al., 2002: Parameterization of wind gustiness for the computation of ocean surface fluxes at different spatial scales, *Mon. Wea. Rev.*, **130**(8), 2125–2133.
- Zhou, T., B. Wu, A. A. Scaife, et al., 2009a: The CLIVAR C20C Project: Which components of the Asian-Australian monsoon circulation variations are forced and reproducible? *Climate Dyn.*, **33**, 1051–1068, doi:10.1007/s00382-008-0501-8.
- Zhou, T., B. Wu, and B. Wang, 2009b: How well do atmospheric general circulation models capture the leading modes of the interannual variability of Asian-Australian Monsoon? *J. Climate*, **22**, 1159–1173.
- Zhou, T., R. Yu, J. Zhang, et al., 2009c: Why the western Pacific subtropical high has extended westward since the late 1970s? *J. Climate*, **22**, 2199–2215.